Artificial Intelligence In Medicine 102 (2020) 101756

Contents lists available at ScienceDirect

Artificial Intelligence In Medicine

journal homepage: www.elsevier.com/locate/artmed

Skin cancer diagnosis based on optimized convolutional neural network

Ni Zhang[a], Yi-Xin Cai[a], Yong-Yong Wang[a], Yi-Tao Tian[a], Xiao-Li Wang[b,*], Benjamin Badami[c]

[a] Department of Throracic Surgery, Tongji Hospital, Tongji Medical College, Huazhong University of Science and Technology, 1095 Jiefang Avenue, Wuhan, Hubei 430030, China
[b] Cancer Biology Research Center, Tongji Hospital, Tongji Medical College, Huazhong University of Science and Technology, Wuhan, Hubei 430030, China
[c] University of Georgia, Athens, USA

ARTICLE INFO

Keywords:
Skin cancer diagnosis
Deep learning
Convolutional neural networks
Whale optimization algorithm
Lévy flight

ABSTRACT

Early detection of skin cancer is very important and can prevent some skin cancers, such as focal cell carcinoma and melanoma. Although there are several reasons that have bad impacts on the detection precision. Recently, the utilization of image processing and machine vision in medical applications is increasing. In this paper, a new image processing based method has been proposed for the early detection of skin cancer. The method utilizes an optimal Convolutional neural network (CNN) for this purpose. In this paper, improved whale optimization algorithm is utilized for optimizing the CNN. For evaluation of the proposed method, it is compared with some different methods on two different datasets. Simulation results show that the proposed method has superiority toward the other compared methods.

1. Introduction

The skin is the broadest organ in the body which protects the body against the heat, light, and infection. It also helps to control the body temperature and to store the fat and the water. One of the most important problems of skin in the body is its infection risk to skin cancer [1].

Skin cancer starts from the cells - the main components that make up the skin - the skin cells grow and divide to form new cells. Everyday skin cells grow old and die and new cells take their place. Sometimes this systematic process does the wrong thing. New cells are created when the skin does not need them, and old cells die when they do not have to. These extra cells form a mass of tissue called a tumor [2,3].

Melanoma is the most malignant and most serious type of skin cancer and is the reason for most deaths from skin cancer. The underlying cause of melanoma is unknown [4]. But several factors, including genetic factors, ultraviolet radiation, and environmental contact are involved in causing the disease.

Melanoma originates from skin melanocytes that have undergone malignant transformation. Melanocytes produce dark pigments on the skin, hair, eyes, and spots of the body. Therefore, melanoma tumors are mostly brown or black. But in a few cases, melanomas do not produce pigment and appear pink, red or purple [5].

Melanoma is the 19th most commonly happening cancer among the humankind such that about 300,000 new cases have been found in 2018. On average, 2490 females and 4740 males lost their lives due to melanoma during 2019 [6]. Fig. 1 illustrates the top 20 countries with the highest melanoma rates in 2018 [7].

However the chance of healing of this cancer is high, it is still counted as a major concern of people due to its high prevalence [8]. Sometimes, melanoma spread through the lymphatic system or circulatory system and achieve the farthest points of the body [9]. This cancer has the highest rate of probability among various kinds of skin cancer [10–14]. Studies have shown that the early detection of melanoma helps significantly to reduce the death rate of melanoma cancer [15]. A significant problem is that the early diagnosis of melanoma, even by specialists, is a hard-core process. Therefore, using a method for simplifying the diagnosis can be helpful for the specialists [16–19].

In the recent decade, the application of image processing and machine vision for different usage of medical imaging is exponentially increasing [20–22]. Using these techniques increases the diagnosis process speed and decreases human errors. It can also improve the quality and the convenience of the melanoma diagnosis by the physicians and radiologists.

For instance, in 2016, Pennisi et al. [23] proposed a melanoma image segmentation basedon delaunay triangulation.

The method was automated melanoma detection. They analyzed the method on a publicly available dermoscopic images benchmark. Final results showed a sensitivity of 93.5 % for the proposed method.

In 2018, Heller et al. [24] proposed a method based on

* Corresponding author.
E-mail address: xiaoliwangcn@163.com (X.-L. Wang).

https://doi.org/10.1016/j.artmed.2019.101756
Received 4 March 2019; Received in revised form 1 October 2019; Accepted 5 November 2019

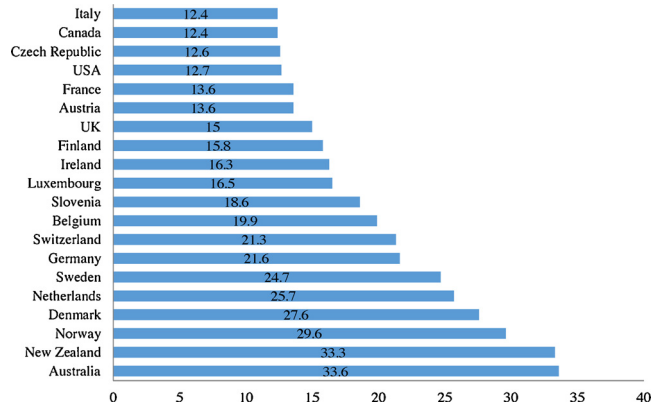

Fig. 1. The age-standardised rate of melanoma in 2018 [7].

morphological features for melanoma detection. The method determined a computer-aided diagnosis system for skin cancer detection.

Artificial Neural Network (ANN) is a part of Artificial Intelligence that can be used in different applications of image processing, like image segmentation and image classification [21,25–30]. For example, in 2016, Kanimozhi et al. [31] proposed a method based on artificial neural networks for skin cancer diagnosis.

The method used Asymmetry, Border, Color, Diameter, (ABCD rule) for better cancer analysis. Results showed about 97 % accuracy for the training of neural network. The method is then used for testing the cancer classification. Final experiments showed the system proper efficiency.

Deep convolutional neural networks (CNNs) is a new different type of artificial neural networks which gives strong results for general and highly variable tasks in different image processing applications. In recent years there are some different applications of deep neural networks for medical imaging [32]. For example, Esteva et al. [33] proposed a dermatologist-level classification for melanoma based on deep neural networks. They used CNN for the classification of melanoma using a single CNN, by directly training end-to-end from images. The method efficiency was testified toward 21 board-certified dermatologists on biopsy-proven clinical images.

Due to the high precision of the CNNs, they have a lot of applications in different parts of medical imaging such as MR images fusion [34], lesion classification [35], tumor diagnosis [36], breast cancer [37], and panoptic analysis [38]. For the explained methods based on CNN, the image was first divided into several small superpixels and then the operator was applied to each of the superpixels. Based on the aforementioned literature, it is concluded that the use of CNN models develops the efficiency of the diagnosis system [39]. One other method for improving the efficiency of the system is to combine them by optimization algorithms [40].

Generally, the applications of using optimization algorithms in different fields of science and engineering are increasing. A new optimization algorithm for solving these kinds of problems is the whale optimization algorithm which is introduced by Mirjalili and Lewis in 2016 [41]. The whale optimization algorithm inspires the process of bubble-net hunting in humpback whales for trapping the prey [42–46].

This study presents a new technique of using an improved whale optimization algorithm for skin cancer detection. Indeed, the main idea here is to utilize the improved whale optimization algorithm to enhance a Convolutional neural network with higher efficiency for the diagnosis usages.

The next sections of the paper are as follows. In Section 2, the concept of Convolutional Neural Networks is explained. Section 3 represents an improved whale optimization algorithm. Section 4 is about how the neural network is optimized by the optimization algorithm. Section 5 describes the employed datasets for system performance analysis. Section 6 includes the algorithm implementation on the case studies and the paper is concluded in Section 7.

2. Convolutional neural networks

The Convolutional Neural Networks (CNN) is an improved type of neural network that is developed by Yann LeCun, et al. [47]. CNN can be adopted for utilizing different mathematical learning methods like regularization, backpropagation, and gradient descent [13,48]. CNN contains three principal concepts of layers including Convolutional layer, pooling layer, and fully connected layer.

Due to the high performance of the artificial neural networks, they are known as proper solutions of several complex problems in image processing and machine vision. A drawback feature of these networks is that the multilayer perceptron models and other similar networks adopted gradient descent for minimizing the error between the achieved response from the network and the desired value. Indeed, sometimes using gradient descent, the solution stuck in the local minimum and doesn't give the best global solution.

CNN is very efficient for solving complex problems [49]. In CNN, the Convolution layer includes a large number of weights which are sub-sampled by pooling layer to give output from convolution layer and decrease data ratio of the layer below. Finally the outputs of the pooling layer are utilized to be injected into the fully connected layers. An important part of CNN is Convolutional neuron layers that include different data for different applications such as image classification and multiple 2D matrices. Since there is no fixed method about determining the number of inputs and output.

This mechanism can extract the regional characteristics of the original image based on the local features extraction. The main idea behind the learning procedure is to achieve some kernel matrices for generating better prominent features for the problem (here skin cancer diagnosis). Here, the backpropagation (BP) approach has been used for achieving the minimum value of the error for the network. Sliding window based convolution is utilized here for the network.

In this study, the rectified linear unit (ReLU) is utilized as the activation function for the neurons by a function $f(x) = \max(x, 0)$ [50]. Max pooling is also adopter for more scale reduction of the network output such that just the highest values are considered as the subsequent layer of the sliding grid.

BP approach is a gradient descent based algorithm for minimizing the error of the neural network based on minimizing the cross-entropy loss as the fitness function [51]. This conception can be described as follows.

$$L = \sum_{j=1}^{N} \sum_{i=1}^{M} -d_j^{(i)} \log z_j^{(i)} \tag{1}$$

where, N is the number of samples, $d_j = (0, \ldots, 0, \underbrace{1, \ldots, 1}_{k}, 0, \ldots, 0)$ is the desired output vector and z_j is the obtained output vector of the m^{th} class which can be achieved by the following formula:

$$z_j^{(i)} = \frac{e^{f_j}}{\sum_{i=1}^{M} e^{f_i}} \tag{2}$$

The weight penalty is adopted for developing the function L to include a η value to improve the values of the weights:

$$L = \sum_{j=1}^{N} \sum_{i=1}^{M} -d_j^{(i)} \log z_j^{(i)} + \frac{1}{2} \eta \sum_K \sum_L \omega_{k,l}^2 \tag{3}$$

where, ω_k represents the connection weight, L is the total number of layers and K is the layer l connections.

Fig. 2 shows a block diagram of an ordinary CNN for skin cancer detection.

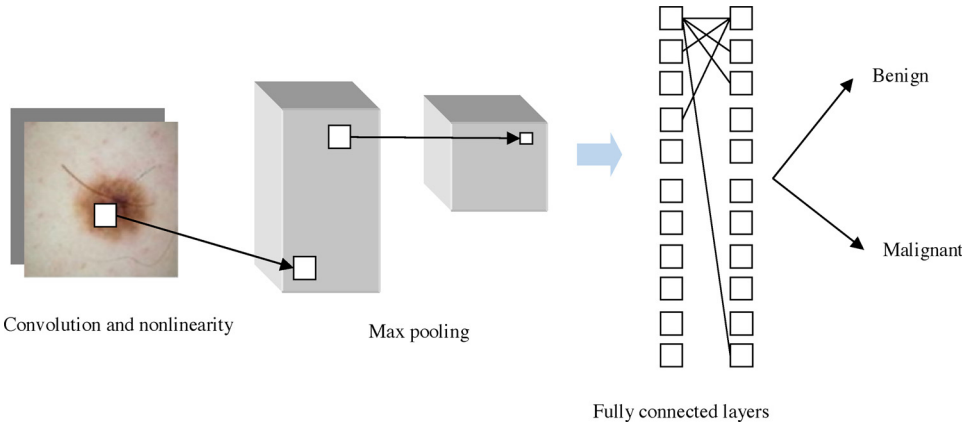

Fig. 2. A simple skin cancer detection using ordinary CNN.

3. Improved whale optimization algorithm based on Lévy flight

In 2016, Mirjalili et al. [41] proposed a new meta-heuristic technique, called Whale optimization algorithm (WOA) that is inspired by the hunting process of the whales [41]. It starts by a number of random candidates solution vectors to achieve find the global optimum of the problem. In the following, some details of this algorithm have been explained.

3.1. Improved whale optimization algorithm

The algorithm continues until the termination criteria has been satisfied. The main concept of WOA is about how the whales can trap the prey based on *bubble-net mechanism with their* spiral movements.

The humpback whale creates bubble nets around the prey which circumvent them into a spiral area. Then it attacks the prey. The mathematical formulation for bubble-net hunting is given below:

$$X_{i+1} = \begin{cases} X_i^*(t) - AD & p < 0.5 \\ D' e^{bl} \cos(2\pi t) + X_i^*(t) & p \geq 0.5 \end{cases} \tag{4}$$

$$D'_i = |CX_i^*(t) - X_i(t)| \tag{5}$$

$$A = 2ar - a \tag{6}$$

$$C = 2r \tag{7}$$

where, i represents the current iteration, l describes a random constant between -1 and 1, p and r are two random constants between 0 and 1, b is the logarithmic shape of the spiral motion, D' describes the distance for the i^{th} whale from the prey (the best solution), and a descent from 2 to 0 linearly over the iteration.

In the above equation, X_{i+1} is the formulation of the encircling process and the second term is the model of the bubble-net process. In WOA, X_{i+1} and D' model the exploration and the exploitation [41]. In WOA, for ensuring the global optimum, the absolute of X should be greater than 1. A principal drawback of the WOA is its premature convergence [52]. In this part, a method is proposed for improving the algorithm efficiency.

3.2. Lévy flight mechanism

In this section, we utilized the function Lévy flight (LF) employed in [52] for developing the presented WOA. This term is adopted for more relieve the premature convergence drawback that is the main drawback in the WOA. *LF* provides a random walk mechanism to proper control of local search [53]. This mechanism is represented as follows:

$$LF(t) \approx t^{-(1+\vartheta)} \tag{8}$$

$$t = \frac{\alpha}{|\beta|^{1/\vartheta}}, \quad \alpha, \beta \sim N(0, \sigma^2) \tag{9}$$

$$\sigma^2 = \left[\frac{\Gamma(1+\vartheta)}{\vartheta \Gamma((1+\vartheta)/2)} \frac{\sin(\pi\vartheta/2)}{2^{(1+\vartheta)/2}} \right]^{\frac{2}{\vartheta}} \tag{10}$$

where, t describes the step size, $\Gamma(.)$ is Gamma function, ϑ represents Lévy index, and A/B $\sim$ N(0, σ^2).

In this paper, based on [54], $\vartheta = 3/2$.

The new improved part for updating the solution of WOA is as follows:

$$\tilde{X}_{i+1} = \begin{cases} X_{i+1} + (X_i^*(t) - AD) \times LV(t) & p < 0.5 \\ X_{i+1} + (D' e^{bl} \cos(2\pi t) + X_i^*(t)) \times LV(t) & p \geq 0.5 \end{cases} \tag{11}$$

where, $\tilde{X}_{i+1}$ describes the new position of search agent X_{i+1}.

Then fitter agents are kept to guarantee the best solution as follows:

$$\tilde{X}_{i+1} = \begin{cases} \tilde{X}_{i+1} & F(\tilde{X}_{i+1}) > F(X_{i+1}) \\ X_{i+1} & O.W. \end{cases} \tag{12}$$

The flowchart of the presented WOA is given in Fig. 3.

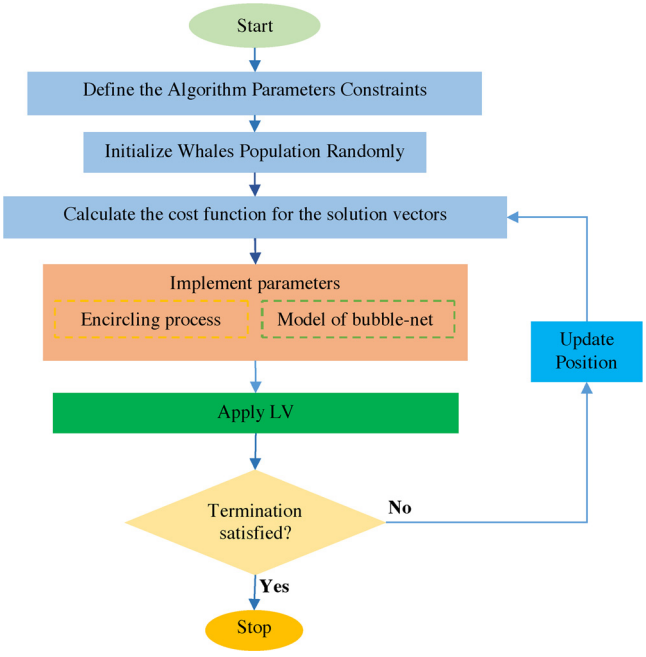

Fig. 3. The block diagram of the Improved WOA.

Table 1
The utilized standard benchmarks that have been utilized for the comparison.

Benchmark	Formula	Constraints	Dimension
Rastrigin	$f_1(x) = 10D + \sum_{i=1}^{D} (x_i^2 - 10\cos(2\pi x_i))$	[−512, 512]	30–50
Rosenbrock	$f_2(x) = \sum_{i=1}^{D-1} (100(x_i^2 - x_{i+1}) + (x_i - 1)^2)$	[−2.045, 2.045]	30–50
Ackley	$f_3(x) = -20\exp\left(-0.2\sqrt{\frac{1}{D}\sum_{i=1}^{D} x_i^2}\right) - \exp\left(\frac{1}{D}\sum_{i=1}^{D}\cos(2\pi x_i)\right) + 20 + e$	[−10, 10]	30–50
Sphere	$f_4(x) = \sum_{i=1}^{D} x_i^2$	[−512, 512]	30–50

Table 2
The optimization results of the different algorithms for validation by considering 30-dimensions.

Benchmark		*Improved WOA*	GA [57]	PSO [59]	WCO [42]	WOA
f_1	MD	0.00	70.61	74.24	2.19	2.23
	SD	0.00	1.66	8.96	4.35	3.19
f_2	MD	7.62	35.41	200.1	13.16	12.93
	SD	2.15	27.15	59.00	4.62	4.96
f_3	MD	0.00	3.19e-2	8.26	3.14e-3	7.25e-15
	SD	0.00	2.14e-2	1.19	1.12e-3	0.00
f_4	MD	0.00	1.15e-4	8.27e-4	6.19e-9	0.00
	SD	0.00	3.14e-5	5.12e-4	3.28e-9	0.00

3.3. The algorithm validation

To analysis and validating the efficiency of the improved IWO, it is compared with some different algorithms such as genetic algorithm (GA) [57], shark smell optimization (SSO) algorithm [38], world cup optimization algorithm (WCO) [42], the original grasshopper optimization algorithm (GOA) [58], and particle swarm optimization algorithm (PSO) [59]. Table 1 illustrates the utilized standard benchmarks that have been utilized for the comparison.

Table 2 illustrates the simulation results of the different algorithms on the adopted benchmarks. As can be seen, the optimal value for the proposed method such that the mean deviation (MD) and the standard deviation (SD) values can win all the algorithms.

This superiority has been made due to adopting logistic mechanism in the algorithm (Fig. 4).

4. Optimized CNN

There are different research works which have been utilized for optimizing the structure of the CNN. Especially, the utilization of the optimization algorithms in CNNs showed promising results [55]. In this study, a new optimized method is proposed for optimizing the structure of CNN. Fig. 5 shows the architecture of the proposed Convolution neural network. The size of input images in the input is considered 28 × 28 pixel.

In this problem, the parameter “max” as the size of the sliding window and the parameter “min” as the minimum value that is acceptable for the max-pooling minimum (and is considered 2 here) to decrease the system error. It should be noted that the value of the sliding window should be less than the input data. Then, a set of solutions have been randomly achieved.

The main purpose of CNN training is to achieve better results for layer parameters which establish a good relationship between the layers to guarantee the proper identification. As aforementioned, in ordinary CNN, the gradient descent algorithm is utilized to optimize the model parameters including convolution filters and the fully connected layers weights. Because of the importance of last layer in classification results, it is important to assign the image into related class which is done by correct connection of the weights with the previous layers. To develop the classification accuracy here, it is attempted to optimize the training of the last weight vector based on the proposed improved whale optimization algorithm. The number of search agents is set 50, maximum number of iteration is considered 100, and the last parameter (vector *a*) is changed linearly in [0,2]. The fitness function for minimizing CNN is considered as follows:

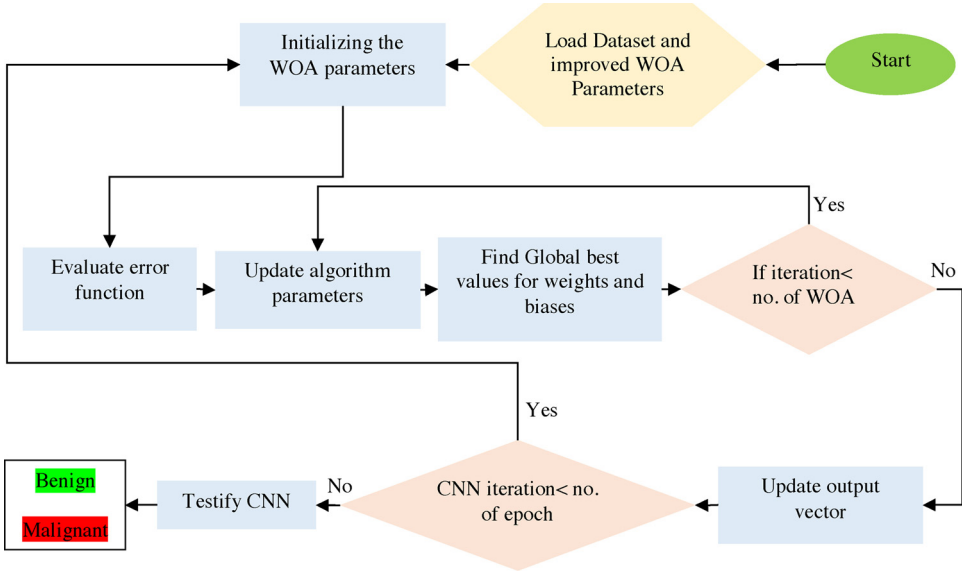

Fig. 4. The Block diagram of the proposed algorithm.

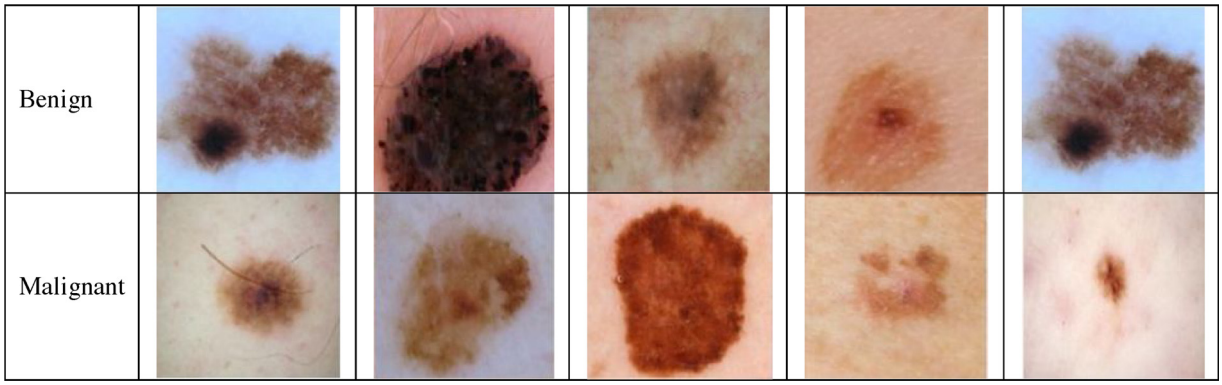

Fig. 5. Some samples of benign and malignant skin cancer images from Dermquest and DermIS databases.

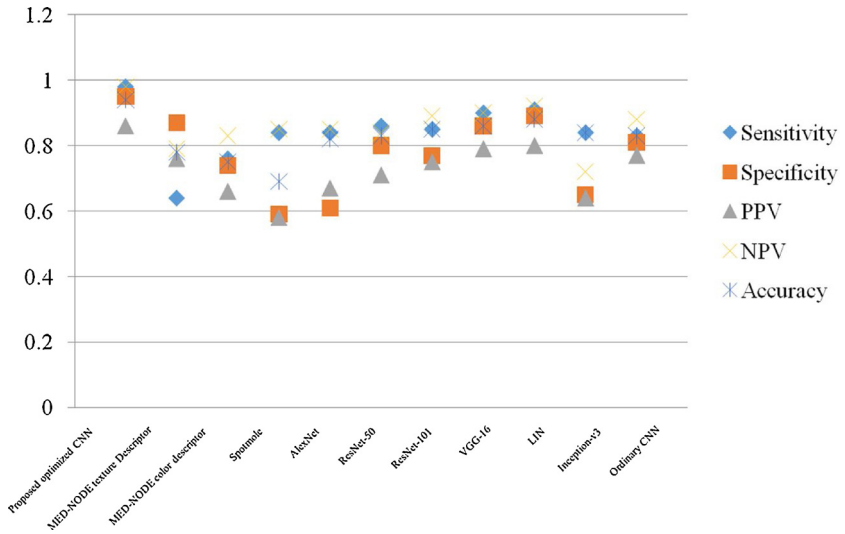

Fig. 6. The performance analysis of the proposed method and the other compared methods with 45 times repetitions.

$$E = \frac{1}{T}\sum_{i=1}^{n_t}\sum_{j=1}^{n_{ol}}(D_{ji} - O_{ji})^2 \tag{13}$$

where, D_{ji} and O_{ji} are the desired value and the CNN output value, n_t represents the number of training samples, and n_{ol} describes the number of output layers.

After determining the parameters of the algorithms, it is applied to CNN. In this study, half-value precision function is utilized for validation of the optimized skin cancer system. After parameter initialization and evaluating the function value, the algorithm parameters have been updated using the parameters such as bubble net hunting and prey enriching. The updating process repeats until the termination criteria have been obtained. The designed system is then analyzed and tested on two different databases, Dermquest, and DermIS databases by considering the MSE minimization. Weights and biases are important parameter of the CNN which have been optimized in this research, these two features have been selected for optimizing as follows:

$$b_n = \{b_{1n}, b_{2n}, ..., b_{Ln}\}$$
$$l = 1, 2, ..., L$$
$$n = 1, 2, ..., A \tag{14}$$

$$A = \{a_1, a_2, ..., a_A\} \tag{15}$$

$$w_n = \{w_{1n}, w_{2n}, ..., w_{Ln}\} \tag{16}$$

where, A describes the total number of agents, l represents the layer index, L is the total number of layers, n is the number of the agent, and w_{in} represents the value of the weight in layer i.

Therefore, the total parameters for optimizing are both weights and biases (i.e. $W_n = \{W, A\}$).

The reason for using improved WOA instead of BP for Error minimization is that the improved WOA doesn't need to backward.

5. The dataset

The data sets used in this study are the Dermquest [56] and DermIS [57] Digital Database. Dermquest database is an online medical atlas for dermatologist and dermatologists based healthcare professionals. The images in Dermquest are reviewed and approved by the re-known international editorial boards. It provides an extensive number of dermatologists including over 22,000 clinical images.

Another database, DermIS Digital Database is an image atlas about different kinds of skin cancers with differential diagnoses that are launched for medical image processing applications. DermIS is accounted as the largest online information service available on the Internet. Some samples of the databases are shown in Fig. 5.

6. Implementation results

In this section, the experimental results of the proposed system have been applied to the databases to analyze the system efficiency. The software for simulation is Matlab R2016® and the hardware configuration is an Intel Core i7 − 4790 K processor with 64 GB of RAM, and two NVIDIA GeForce GTX Titan X GPU cards with scalable link interface (SLI).

In this study, two classes including the background region and the cancerous region have been considered. A set of 3 × n vector including

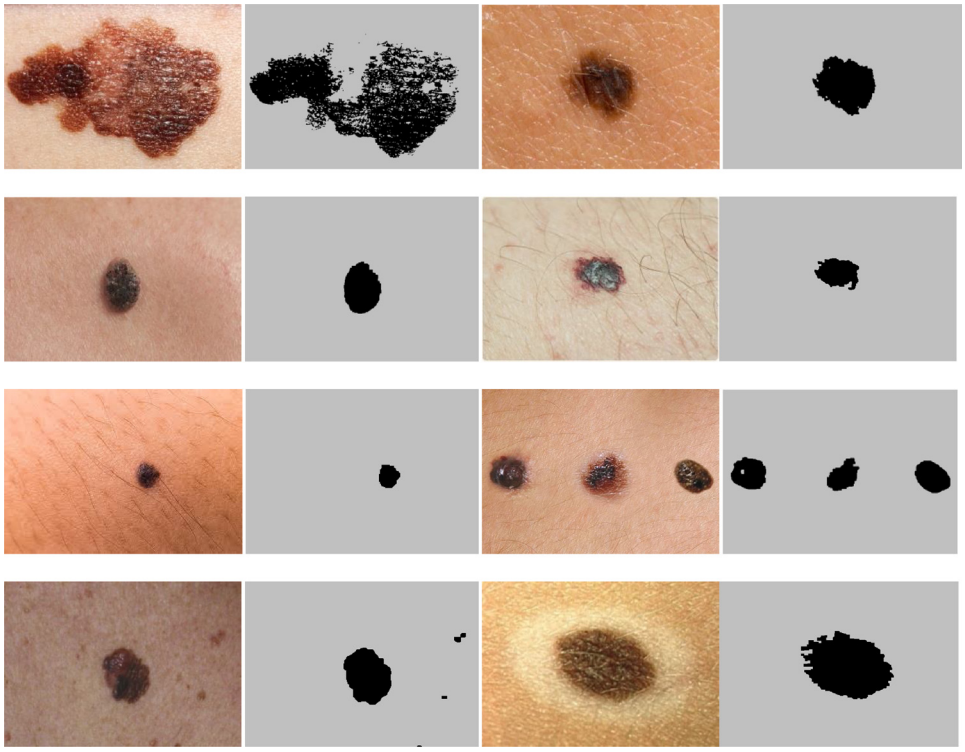

Fig. 7. Some examples of applying the proposed optimized CNN: input images and detected masks.

pixel color features (R, G, and B information) of the image has been considered. The selected transfer function for the Convolutional neural network is rectified linear unit (ReLU).

Simulations have been applied to two different benchmarks including Dermquest and DermIS for performance analysis of the proposed method. The proposed optimized CNN here is trained and testified on the dataset. In this study for the proposed optimized CNN network, 80 % of the dataset has been selected for the training and 20 % have been selected for the testing. 28,000 iterations have been considered for training the optimized CNN. To make an independent analysis, the training step is repeated 45 times and the results have been considered based on mean value of these results. Five performance indexes have been served for the method analysis.

$$Specifity = \frac{correctly\ detected\ healthy\ skin\ cases}{Total\ healthy\ skin\ cases} \tag{17}$$

$$Sensitivity = \frac{correctly\ detected\ skin\ cancer\ cases}{Total\ skin\ cancer\ cases} \tag{18}$$

$$accuracy = \frac{correctly\ detected\ cases}{total\ cases} \tag{19}$$

$$NPV = \frac{correctly\ detected\ healthy\ skin\ cases}{detected\ healthy\ skin\ cases} \tag{20}$$

$$PPV = \frac{correctly\ detected\ skin\ cancer\ cases}{detected\ skin\ cancer\ cases} \tag{21}$$

In this paper, the results of the proposed optimized CNN are compared with some different state of the art methods for illustrating the system efficiency. These algorithms are including a framework based on the semi-supervised system [58], a commercial tool [59], and some deep methods such as AlexNet [60], Ordinary CNN, VGG-16 [61], LIN [62], Inception-v3 [63], and ResNet [64]. The performance analysis of the proposed method and the other compared methods are given in Fig. 6.

Form the figure, it can be concluded that the proposed optimized method has the highest value of the specificity, accuracy, sensitivity, NPV, and PPV. Final results illustrate that using the proposed WOA on CNN gives the best achievements toward the compared methods.

Some examples of applying the proposed optimized CNN are shown in Fig. 7. As can be seen, using the proposed network for skin cancer diagnosis not only can segment the lesions in the standard databases but also can detect the lesion in the images with artifacts like body hair. Simulation results showed that the performance of the proposed method is good enough for the skin cancer diagnosis in different environmental conditions.

7. Conclusions

In the present study, a new optimized technique was proposed for skin cancer diagnosis from the input images. The method was based on Convolutional neural network. An improved version of the whale optimization algorithm was adopted for optimizing the efficiency result of CNN. The utilized optimization algorithm is adopted for the optimal selection of weights and biases in the network to minimize the error of the network output and the desired output. For performance analysis of the proposed method, it is tested on two different benchmarks including Dermquest and DermIS and the results were compared with 10 different methods including semi-supervised method, Spot-mole tool, AlexNet, Ordinary CNN, VGG-16, LIN, Inception-v3, and ResNet. The performance indexes here are specificity, accuracy, sensitivity, NPV, and PPV. Final results showed that using the proposed method gives the best achievement for the skin cancer diagnosis.

Acknowledgments

This project was supported by a grant from the National Natural Sciences Foundation of China (No.81802602).

References

[1] Byrd AL, Belkaid Y, Segre JA. The human skin microbiome. Nat Rev Microbiol 2018;16:143.
[2] O'Sullivan DE, Brenner DR, Demers PA, Villeneuve PJ, Friedenreich CM, King WD,

et al. Indoor tanning and skin cancer in Canada: a meta-analysis and attributable burden estimation. Cancer Epidemiol 2019;59:1–7.
[3] Hylands P. Skin cancer: types, diagnosis and prevention. Heart Fail 2019;10. p. 00.
[4] Martínez YJ, Alcalá GR, Ortega MBG, López-Ruiz E, Jiménez G, Marchal JA, et al. Melanoma cancer stem-like cells: optimization method for culture, enrichment and maintenance. Tissue Cell 2019.
[5] Hodis E. The somatic genetics of human melanoma. 2018.
[6] Siegel RL, Miller KD, Jemal A. Cancer statistics. CA Cancer J Clin 2019;2019.
[7] Skin cancer statistics: melanoma of the skin is the 19th most common cancer worldwide. 2019 Available: https://www.wcrf.org/dietandcancer/cancer-trends/skin-cancer-statistics.
[8] Force UPST. Behavioral counseling to prevent skin cancer: US Preventive Services Task Force recommendation statement. JAMA-J Am Med Assoc 2018;319:1134–42.
[9] Al-Jamal RaT, Cassoux N, Desjardins L, Damato B, Konstantinidis L, Coupland SE, et al. The pediatric choroidal and ciliary body melanoma study a survey by the european ophthalmic oncology group. Ophthalmology 2016.
[10] Codella N, Cai J, Abedini M, Garnavi R, Halpern A, Smith JR. Deep learning, sparse coding, and SVM for melanoma recognition in dermoscopy images. in International Workshop on Machine Learning in Medical Imaging 2015:118–26.
[11] Dalila F, Zohra A, Reda K, Hocine C. Segmentation and classification of melanoma and benign skin lesions. Opt – Int J Light Electron Opt 2017;140:749–61.
[12] Cai Wei, et al. Optimal bidding and offering strategies of compressed air energy storage: a hybrid robust-stochastic approach. Renew Energy 2019;143:1–8.
[13] Razmjooy N, Sheykhahmad FR, Ghadimi N. A hybrid neural network–world cup optimization algorithm for melanoma detection. Open Med 2018;13:9–16.
[14] Silveira M, Nascimento JC, Marques JS, Marçal AR, Mendonça T, Yamauchi S, et al. Comparison of segmentation methods for melanoma diagnosis in dermoscopy images. IEEE J Sel Top Signal Process 2009;3:35–45.
[15] Razmjooy N, Mousavi BS, Soleymani F. A real-time mathematical computer method for potato inspection using machine vision. Comput Math Appl 2012;63:268–79.
[16] Cohen VM, Pavlidou E, DaCosta J, Arora AK, Szyszko T, Sagoo MS, et al. Staging uveal melanoma with whole-body positron-emission tomography/computed tomography and abdominal ultrasound: low incidence of metastatic disease, high incidence of second primary cancers. Middle East Afr J Ophthalmol 2018;25:91.
[17] Khodaei Hossein, et al. Fuzzy-based heat and power hub models for cost-emission operation of an industrial consumer using compromise programming. Appl Therm Eng 2018;137:395–405.
[18] Kulkarni A, Mukhopadhyay D. SVM classifier based melanoma image classification. Res J Pharm Technol 2017;10:4391–2.
[19] Narasimhan K, Elamaran V. Wavelet-based energy features for diagnosis of melanoma from dermoscopic images. Int J Biomed Eng Technol 2016;20:243–52.
[20] El-Regaily SA, Salem MA, Abdel Aziz MH, Roushdy MI. Survey of computer aided detection systems for lung cancer in computed tomography. Curr Med Imaging Rev 2018;14:3–18.
[21] Razmjooy N, Mousavi BS, Soleymani F. A hybrid neural network Imperialist Competitive Algorithm for skin color segmentation. Math Comput Model 2013;57:848–56.
[22] Mohan G, Subashini MM. MRI based medical image analysis: survey on brain tumor grade classification. Biomed Signal Process Control 2018;39:139–61.
[23] Gao Wei, et al. Different states of multi-block based forecast engine for price and load prediction. Int J Electr Power Energy Syst 2019;104:423–35.
[24] Heller N, Bussman E, Shah A, Dean J, Papanikolopoulos N. Computer aided diagnosis of skin lesions from morphological features. 2018.
[25] Mirjalili S. Genetic algorithm. Evolutionary algorithms and neural networks. Springer; 2019. p. 43–55.
[26] Moallem P, Razmjooy N. A multi layer perceptron neural network trained by invasive weed optimization for potato color image segmentation. Trends Appl Sci Res 2012;7:445.
[27] Razmjooy N, Ramezani M. Training wavelet neural networks using hybrid particle swarm optimization and gravitational search algorithm for system identification. 2019.
[28] Such FP, Madhavan V, Conti E, Lehman J, Stanley KO, Clune J. Deep Neuroevolution: Genetic Algorithms are a Competitive Alternative for Training Deep Neural Networks for Reinforcement Learning arXiv preprint arXiv:1712.06567 2017.
[29] Liu Yang, Wang Wei, Ghadimi Noradin. Electricity load forecasting by an improved forecast engine for building level consumers. Energy 2017;139:18–30.
[30] Ghadimi N, Akbarimajd A, Shayeghi H, Abedinia O. Two stage forecast engine with feature selection technique and improved meta-heuristic algorithm for electricity load forecasting. Energy 2018;161:130–42.
[31] Kanimozhi T, Murthi A. Computer aided melanoma skin cancer detection using artificial neural network classifier," Singaporean Journal of Scientific Research (SJSR). J Selected Areas Microelectron (JSAM) 2016;8:35–42.
[32] Xie H, Yang D, Sun N, Chen Z, Zhang Y. Automated pulmonary nodule detection in CT images using deep convolutional neural networks. Pattern Recognit 2019;85:109–19.
[33] Esteva A, Kuprel B, Novoa RA, Ko J, Swetter SM, Blau HM, et al. Dermatologist-level classification of skin cancer with deep neural networks. Nature 2017;542:115.
[34] Zhang L, Yin F, Cai J. A multi-source adaptive MR image fusion technique for MR-Guided radiation therapy. Int J Radiat Oncol Biol Phys 2018;102:e552.
[35] Guerrero R, Qin C, Oktay O, Bowles C, Chen L, Joules R, et al. White matter hyperintensity and stroke lesion segmentation and differentiation using convolutional neural networks. Neuroimage Clin 2018;17:918–34.
[36] Hashemi Farid, Ghadimi Noradin, Sobhani Behrooz. Islanding detection for inverter-based DG coupled with using an adaptive neuro-fuzzy inference system. Int J Electr Power Energy Syst 2013;45(1):443–55.
[37] Adoui ME, Mahmoudi SA, Larhmam MA, Benjelloun M. MRI breast tumor segmentation using different encoder and decoder CNN architectures. Computers 2019;8:52.
[38] Mirzapour Farzaneh, et al. A new prediction model of battery and wind-solar output in hybrid power system. J Ambient Intell Humaniz Comput 2019;10(1):77–87.
[39] Sudharshan P, Petitjean C, Spanhol F, Oliveira LE, Heutte L, Honeine P. Multiple instance learning for histopathological breast cancer image classification. Expert Syst Appl 2019;117:103–11.
[40] Blanco R, Cilla JJ, Malagón P, Penas I, Moya JM. Tuning CNN input layout for IDS with genetic algorithms. International Conference on Hybrid Artificial Intelligence Systems 2018:197–209.
[41] Mirjalili S, Lewis A. The whale optimization algorithm. Adv Eng Softw 2016;95:51–67.
[42] Oliva D, El Aziz MA, Hassanien AE. Parameter estimation of photovoltaic cells using an improved chaotic whale optimization algorithm. Appl Energy 2017;200:141–54.
[43] Kaveh A, Ghazaan MI. Enhanced whale optimization algorithm for sizing optimization of skeletal structures. Mech Based Des Struct Mach 2017;45:345–62.
[44] Mafarja MM, Mirjalili S. Hybrid Whale Optimization Algorithm with simulated annealing for feature selection. Neurocomputing 2017;260:302–12.
[45] El Aziz MA, Ewees AA, Hassanien AE. Whale Optimization Algorithm and Moth-Flame Optimization for multilevel thresholding image segmentation. Expert Syst Appl 2017;83:242–56.
[46] Trivedi IN, Pradeep J, Narottam J, Arvind K, Dilip L. Novel adaptive whale optimization algorithm for global optimization. Indian J Sci Technol 2016;9.
[47] Yosinski J, Clune J, Nguyen A, Fuchs T, Lipson H. Understanding Neural Networks through Deep Visualization arXiv preprint arXiv:1506.06579 2015.
[48] Hamian Melika, et al. A framework to expedite joint energy-reserve payment cost minimization using a custom-designed method based on Mixed Integer Genetic Algorithm. Eng Appl Artif Intell 2018;72:203–12.
[49] Acharya UR, Oh SL, Hagiwara Y, Tan JH, Adeli H. Deep convolutional neural network for the automated detection and diagnosis of seizure using EEG signals. Comput Biol Med 2018;100:270–8.
[50] Koehler F, Risteski A. Representational Power of ReLU Networks and Polynomial Kernels: Beyond Worst-Case Analysis arXiv preprint arXiv:1805.11405, 2018.
[51] Van Merriënboer B, Bahdanau D, Dumoulin V, Serdyuk D, Warde-Farley D, Chorowski J, et al. Blocks and fuel: Frameworks for deep learning. arXiv preprint arXiv:1506.00619. 2015.
[52] Chen H, Xu Y, Wang M, Zhao X. A balanced whale optimization algorithm for constrained engineering design problems. Appl Math Model 2019;71:45–59.
[53] Choi C, Lee J-J. Chaotic local search algorithm. Artif Life Robot 1998;2:41–7.
[54] Leng Hua, et al. A new wind power prediction method based on ridgelet transforms, hybrid feature selection and closed-loop forecasting. Adv Eng Inform 2018;36:20–30.
[55] Xie L, Yuille A. Genetic cnn. Proceedings of the IEEE International Conference on Computer Vision 2017:1379–88.
[56] Database D. Dermquest database Available: 2019https://www.derm101.com/dermquest/.
[57] Xu H, Mandal M. Epidermis segmentation in skin histopathological images based on thickness measurement and k-means algorithm. EURASIP J Image Video Process 2015;2015:18.
[58] Giotis I, Molders N, Land S, Biehl M, Jonkman MF, Petkov N. MED-NODE: a computer-assisted melanoma diagnosis system using non-dermoscopic images. Expert Syst Appl 2015;42:6578–85.
[59] Munteanu C, Cooclea S. Spotmole—melanoma control system. 2009.
[60] Krizhevsky A, Sutskever I, Hinton GE. Imagenet classification with deep convolutional neural networks. Adv Neural Inf Process Syst 2012:1097–105.
[61] Simonyan K, Zisserman A. Very deep convolutional networks for large-scale image recognition. arXiv preprint arXiv:1409.1556. 2014.
[62] Li Y, Shen L. Skin lesion analysis towards melanoma detection using deep learning network. Sensors 2018;18:556.
[63] Szegedy C, Vanhoucke V, Ioffe S, Shlens J, Wojna Z. Rethinking the inception architecture for computer vision. Proceedings of the IEEE Conference on Computer Vision and Pattern Recognition 2016:2818–26.
[64] He K, Zhang X, Ren S, Sun J. Deep residual learning for image recognition. Proceedings of the IEEE Conference on Computer Vision and Pattern Recognition 2016:770–8.